Science of the Total Environment 677 (2019) 599–611

Contents lists available at ScienceDirect

Science of the Total Environment

journal homepage: www.elsevier.com/locate/scitotenv

Quantifying the impacts of dams on riverine hydrology under non-stationary conditions using incomplete data and Gaussian copula models

Denis Valle [a,*], David Kaplan [b]

[a] School of Forest Resources and Conservation, University of Florida, 136 Newins-Ziegler Hall, Gainesville, FL 32611, United States of America
[b] Engineering School of Sustainable Infrastructure & Environment, University of Florida, 102 Phelps Lab, Gainesville, FL 32611, United States of America

HIGHLIGHTS

- We propose and test Gaussian Copula (GC) models for environmental impact assessments.
- The GC model avoids the stationarity assumption and circumvents data gaps.
- This model yielded better predictions than more standard methods.
- We find substantial riverine hydrology alterations associated with the Tucuruí dam.
- Our method is useful to integrate multiple time-series data for impact assessments.

GRAPHICAL ABSTRACT

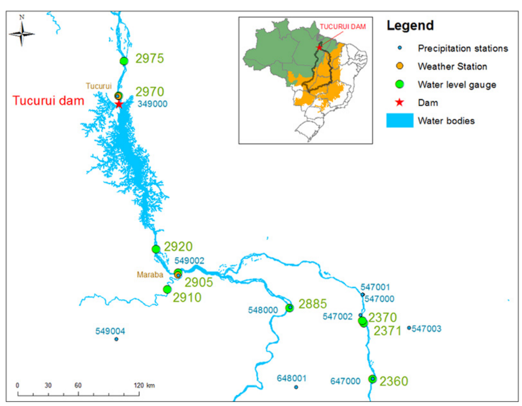

ARTICLE INFO

Article history:
Received 8 January 2019
Received in revised form 8 April 2019
Accepted 25 April 2019
Available online 28 April 2019

Editor: Diego Di Curzio

Keywords:
Impact assessment
Sparse data
Data gap
Stationarity
Counterfactual
Amazon
Dams
Hydrologic alteration

ABSTRACT

Across the world, the assessment of environmental impacts attributable to infrastructure and development projects often require a comparison between observed post-impact outcomes with what "would have happened" in the absence of the impact (i.e., the counterfactual). Environmental impact assessment (EIA) methods traditionally determine the counterfactual based on strong assumptions of stationarity (e.g., using before and after comparisons) and can be particularly challenging to use in the context of substantial data gaps, a vexing problem when combining several time-series data from different sources. Here we propose and test a widely applicable statistical approach for quantifying environmental impacts that avoids the stationarity assumption and circumvents issues associated with data gaps. Specifically, we used a Gaussian Copula (GC) model to assess the hydrological impacts of the Tucuruí dam on the Tocantins River in the Brazilian Amazon.
Using multi-source water level and climate data, GC predictions of pre-dam hydrology for the validation period were excellent (Nash-Sutcliffe coefficients of 0.83 to 0.98 and 93–96% of observations within the 95% predictive intervals). In the post-dam period, the river had higher dry-season water levels both upstream and downstream relative to the predicted counterfactual, and the timing and duration of wet-season drawdown was delayed and extended, substantially altering the flood pulse. These impacts were evident as far as 176 km away from the dam, highlighting widespread hydrological impacts. The GC model outperformed standard multiple regression models in representing predictive uncertainty while also avoiding the stationarity assumption and circumventing the issue of sparse and incomplete data. We thus believe the GC approach has wide utility for integrating disparate time-series data to quantify the impacts of dams and other anthropogenic phenomena on riverine hydrology globally.
© 2019 Elsevier B.V. All rights reserved.

* Corresponding author.
E-mail addresses: drvalle@ufl.edu (D. Valle), dkaplan@ufl.edu (D. Kaplan).

https://doi.org/10.1016/j.scitotenv.2019.04.377
0048-9697/© 2019 Elsevier B.V. All rights reserved.

1. Introduction

Environmental impact assessments typically require a comparison between observed post-impact outcomes with what "would have happened" in the absence of the impact (i.e., the counterfactual). A common approach for determining the counterfactual is to compare variables of interest before and after impact, implicitly assuming that the counterfactual would be similar to what was observed before the impact (i.e., the stationarity assumption). Multiple studies have used this approach to examine the impact of dams on hydrology (e.g., Forsberg et al., 2017; Sabo et al., 2017; Timpe and Kaplan, 2017). Although the assumption of stationarity is central to hydrologic indicator methods (e.g., Richter et al., 1996), it may be invalid when other factors (e.g., climate, land use, and management regimes) have also changed over time, which is often the case when quantifying long-term hydrological impacts (Milly et al., 2007).

A commonly-adopted approach to circumvent the stationarity assumption is the Before-After Control-Impact (BACI) design. With a BACI design, comparable control and treatment sites are identified and monitored before the onset of an impact, after which it is assumed that changes not attributable to the impact influence all sites in a similar fashion. In hydrological studies, BACI designs like the paired watershed approach have greatly advanced our understanding of watershed hydrology (e.g., Clausen and Spooner, 1993; Poff et al., 2007). However, identifying appropriate control sites for BACI designs can be challenging given that they must be close enough to share the effect of concurrent changes while at the same time being distant enough to not be affected by the impact of interest. Furthermore, the assumption that any concurrent change unrelated to the impact will have a similar effect on both control and impact sites may not always hold, particularly over large spatial and temporal scales.

A more recent approach to determining the counterfactual consists of using "synthetic controls". Following the concepts put forth by Abadie et al. (2010), the basic idea consists of creating model-based predictions of the counterfactual based on data from one or more control sites, as well as other potentially important drivers of the phenomenon being studied. As a result, this statistical approach accounts for post-impact changes in important driving variables. However, a critical challenge when applying the synthetic control approach to quantify changes in riverine hydrology is the presence of data gaps in response variables (e.g., discharge or water level time series) as well as their potential drivers (e.g., rainfall, temperature, and evapotranspiration). This "data-gap challenge" is particularly vexing in the developing world (Getirana et al., 2009). Gap-filling algorithms have been proposed and successfully applied in multiple fields, including medicine, hydrology, meteorology, remote sensing, and ecosystem carbon exchange (Andersson et al., 2012; Hui et al., 2004; Ruelland et al., 2008; Schneider, 2001; van Buuren et al., 1999; Weiss et al., 2014). However, none of these methods have focused on predicting the counterfactual, despite the fact that this prediction task can be re-interpreted as a missing data problem (Rubin, 1976).

Given these challenges, we propose to use a Gaussian Copula (GC) model to predict the counterfactual in the presence of substantial data gaps while simultaneously avoiding the stationarity assumption through the integration of data from multiple sources. Copula models have been widely applied in hydrology to quantify the association between multiple hydrological variables, such as drought duration, affected area, and severity (Xu et al., 2015), annual maxima of streamflows or rainfalls (Renard and Lang, 2007), and to predict associations among climate, flows, and flood risk (Favre et al., 2004; Liu et al., 2018; Yin et al., 2018). Despite the widespread use of copula models in hydrology (Hao and Singh, 2016), they have yet to be applied in the context of hydrological impact assessments and in the presence of substantial missing data. Here, we implement the GC approach within a Bayesian framework to fully account for sampling and parameter uncertainty, enabling a statistically rigorous evaluation of how divergent the post-impact hydrologic data are relative to those expected under the modeled counterfactual. We applied the GC model to assess the impact of the Tucuruí dam on the hydrology of the Tocantins River in the Brazilian Amazon. Tucuruí was the first large-scale hydroelectricity project implemented in the Brazilian Amazon, producing 8370 MW of energy and having an inundated reservoir area of 2875 km^2 (Tundisi et al., 2005), and it is emblematic of many of the existing and planned hydroelectric dams in the region (Anderson et al., 2018; Moran et al., 2018).

2. Materials and methods

2.1. Study site and data

The Tocantins River drains 750,000 km^2 of rainforest and savanna (cerrado) in the southeastern Amazon (Fig. 1) and is among the most altered river basins in the Amazon River basin. The first dam on the Tocantins (Tucuruí) came online in 1984 and the second (Serra da Mesa) started to operate in 1998. Today, there are 56 hydroelectric dams in the Tocantins-Araguaia watershed (Castello and Macedo, 2016), with seven large dams on the Tocantins River having an overall published electricity generating capacity of approximately 13,000 MW (i.e., production capacities range from 241 to 8370 Megawatts and reservoir areas range from 104 to 3014 km^2). Two new large dams are planned for the Tocantins and five more are planned or in construction on the Araguaia River (the Tocantins' main tributary) or its tributaries, despite expectations that they will exacerbate harm to regional biodiversity, fisheries, tourism, and indigenous peoples (International Rivers, 2016). Fisheries have been particularly degraded by the cascade of dams on the Tocantins (Cetra and Petrere Jr, 2001; de Mérona et al., 2001; Ribeiro et al., 1995; Tundisi, 2008), promoting new interest in improving our understanding of natural and altered hydrologic regimes in this highly impacted ecosystem.

Water level and precipitation data originally collected by the Brazilian National Water Agency (Agencia Nacional de Aguas; ANA) have been organized and made freely available by Tucker Lima et al. (2016). Other meteorological data (relative humidity, evaporation, minimum, maximum, and mean temperatures) were collected by the Brazilian National Institute of Meteorology (Instituto Nacional de Meteorologia; INMET; freely available at http://www.inmet.gov.br/portal/). These variables were chosen because they are known to strongly influence watershed hydrology (Beighley et al., 2009; Costa and Foley, 1999) and because relatively long time series were available. We only used climate data spanning at least 20 years and water level data spanning (at minimum) the time period between 1975 (the year that construction of Tucuruí began) and 1994 (10 years after Tucuruí began to operate). Given these criteria, our analysis relied primarily on the following 29 variables:

a. Daily water level (cm) from 9 gauges in the Tocantins River and its tributaries;
b. Monthly precipitation (mm) from 10 ground-based stations; and
c. Daily relative humidity (%), daily temperature (minimum, maximum, and mean; °C), and monthly evaporation (mm) from two long-term weather stations (Tucuruí and Marabá)

Daily data were aggregated to monthly averages (sums for precipitation), covering the period from July 1969 to May 2015 (Figs. 2 and 3); these figures illustrate the substantial number of gaps in both water

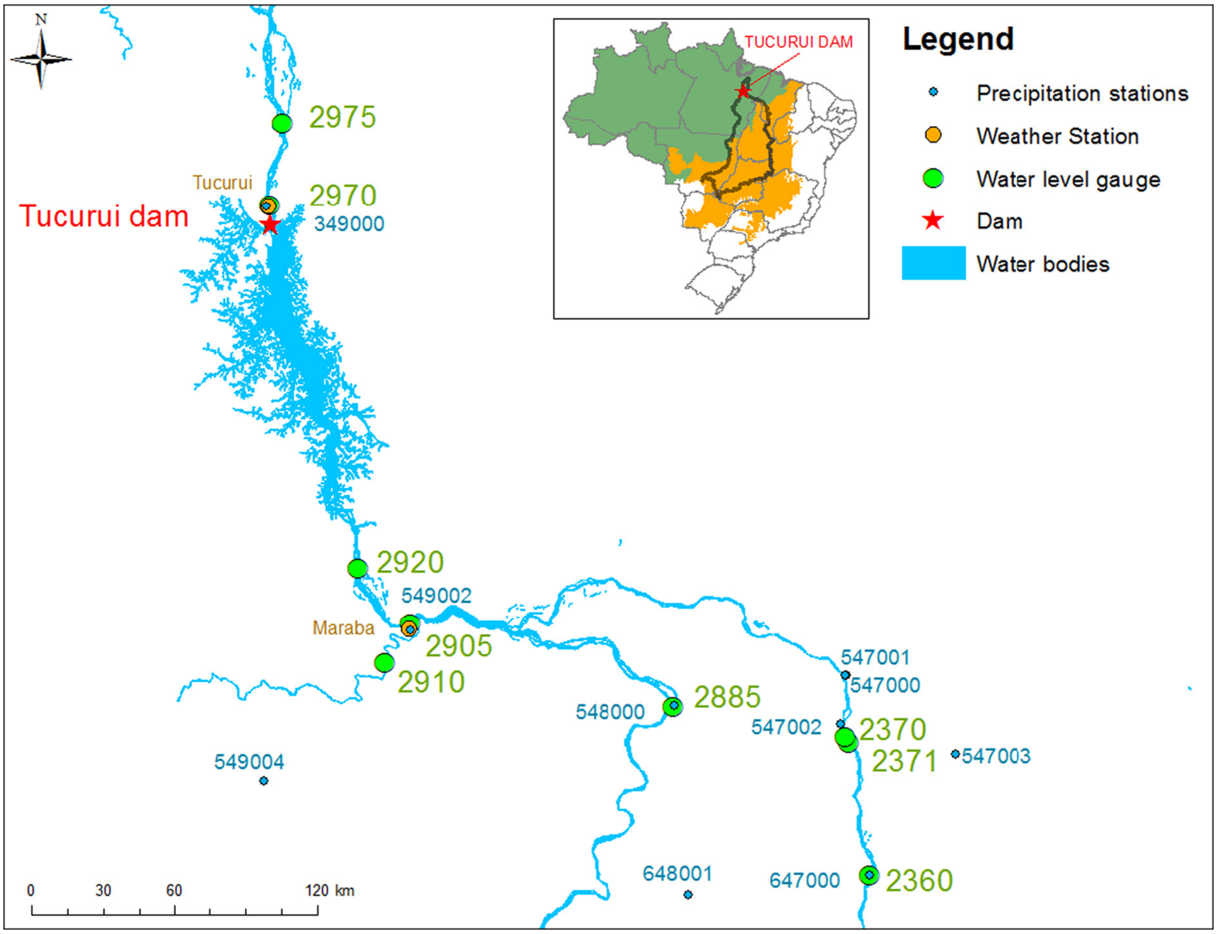

Fig. 1. Location of the Tucuruí dam on Tocantins River in the southeastern Amazon, illustrating the spatial distribution of water level, weather, and precipitation stations used in this study. The identifier for each weather station (orange circle), precipitation station (blue circle), and water level gauge (green circle) are provided in the corresponding color. The Serra da Mesa dam (the second dam to start operating in the Tocantins river) is located approximately 1500 km upstream of Tucuruí and is not shown. Inset displays the extent of the Amazon (green) and Cerrado (orange) biomes, together with the Tocantins and Araguaia watershed boundaries (thick black line) and state limits (grey lines). (For interpretation of the references to color in this figure legend, the reader is referred to the web version of this article.)

level response variables and climate drivers. On average, these time-series had 19% of data missing, though five time-series had >25% missing data.

2.2. Counterfactual period

To create counterfactual predictions, we fit models only to data from sites that have likely not been impacted by any dams. Examination of Fig. 1 suggests that gauges 2970, 2975, and 2920 (and potentially gauges 2905 and 2910) are likely to have been impacted by the Tucuruí dam, an assertion supported by Timpe and Kaplan (2017) in their review of the hydrologic impacts of Amazon dams. Therefore, we excluded data from these gauges from 1984 (the year Tucuruí dam started to operate) onwards (red polygons in Fig. 3). Gauges 2885, 2370, 2371, and 2360, on the other hand, are unlikely to have been impacted by Tucuruí dam given their distance from this dam and their relatively low hydrologic alteration level (Timpe and Kaplan, 2017). Nevertheless, because gauges 2370, 2371, and 2360 might have been impacted from 1998 onwards by the operation of the Serra da Mesa dam and other upstream dams, we excluded their data from 1998 onwards (black polygons in Fig. 3).

We also set the observations from gauges 2975, 2970, 2920, 2905, and 2910 for the pre-impact period between 1979 and 1984 to missing (orange polygons in Fig. 3), allowing us to use this period for model validation. More specifically, we expect that there will be little difference between the predicted and observed water-levels given that no dam had started to operate in the region during this time period. Therefore, we use these data to evaluate the out-of-sample predictive skill of the different models described below (i.e., model validation).

2.3. Multivariate normal distributions

To explain why GC models are useful for impact assessment with sparse data, it is first instructive to review two important properties of the multivariate normal distribution. First, when using multivariate normal distributions, any variable can be predicted with a linear regression model using the other variables as covariates/predictors. For example, assume we have the following model:

$$\begin{bmatrix} z_1 \\ z_2 \\ z_3 \end{bmatrix} \sim N(\boldsymbol{\mu}_{3\times 1}, \boldsymbol{\Sigma}_{3\times 3})$$

where z_1, z_2, z_3 are distinct variables (e.g., water level in gauge 1, water level in gauge 2, and rainfall) and the multivariate normal distribution has mean vector and covariance matrix given by $\boldsymbol{\mu}_{3\times 1} = \begin{bmatrix} \mu_1 \\ \mu_2 \\ \mu_3 \end{bmatrix}$ and $\boldsymbol{\Sigma}_{3\times 3} = \begin{bmatrix} a & b & c \\ b & e & d \\ c & d & f \end{bmatrix}$, respectively. For this model, standard multivariate

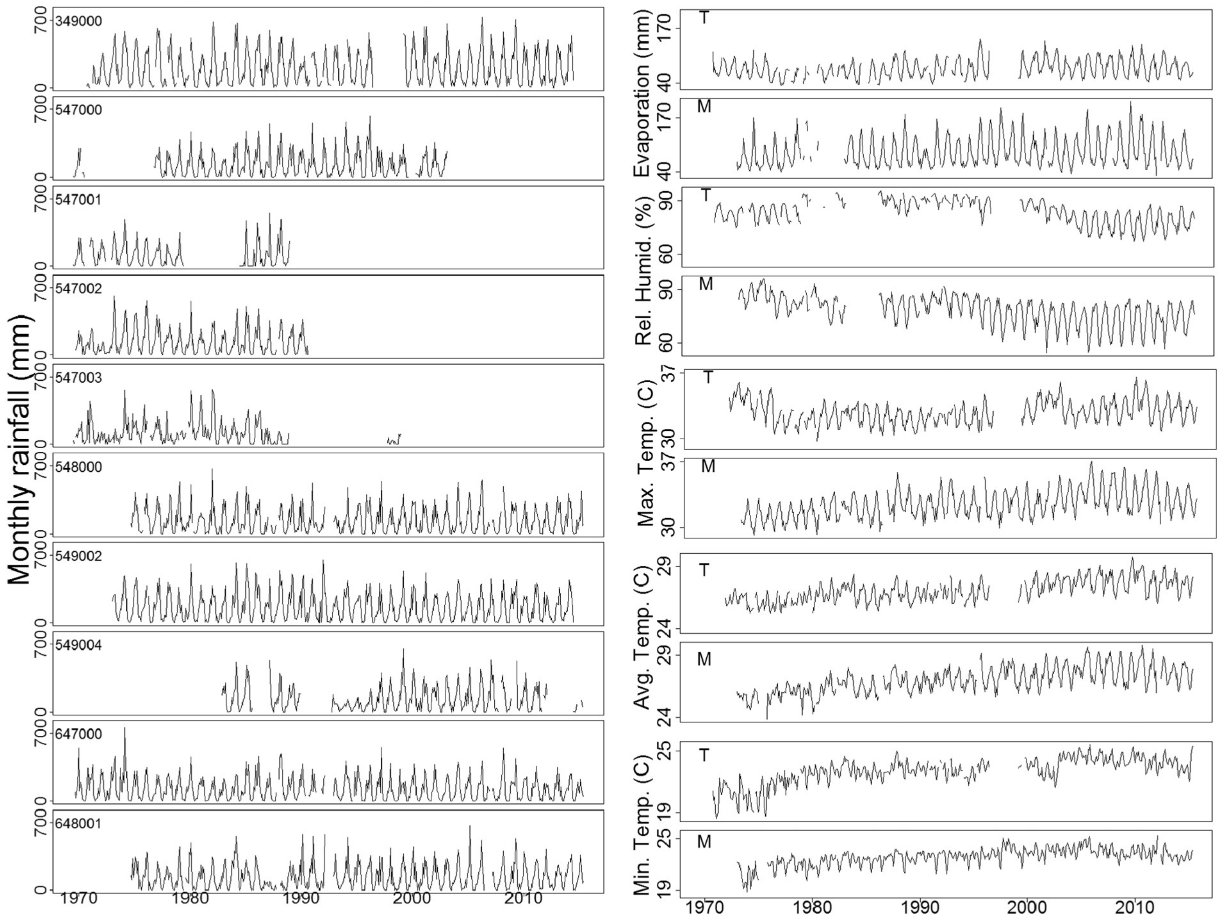

Fig. 2. Time series of climate variables used in this study. Climate variables include rainfall from ten stations (left panels) and evaporation, relative humidity, and temperature (minimum, mean, and maximum) from two weather stations (T and M stand for Tucurui and Maraba, respectively) (right panels). Numbers and names in the top left of each panel refer to station identifiers (see Fig. 1).

normal theory states that:

$$p(z_1|z_2,z_3) = N(\beta_0+\beta_2 z_2+\beta_3 z_3,\sigma^2)$$

where $\beta_0=\mu_1-\frac{bf-cd}{ef-d^2}\mu_2-\frac{ce-bd}{ef-d^2}\mu_3, \beta_2=\frac{bf-dc}{ef-d^2}, \beta_3=\frac{ce-bd}{ef-d^2}, \sigma^2=a-\frac{(bf-dc)b+(ce-bd)c}{ef-d^2}$. This expression illustrates how the assumption of a multivariate normal distribution enables prediction of water level in gauge 1 (z_1) based on data from water level gauge 2 (z_2) and rainfall (z_3) using linear regression.

The second property of multivariate normal distributions that make them useful for our application is that any subset of variables will also have a joint multivariate normal distribution, with the corresponding covariance matrix parameters. Using the example above, if rainfall data (z_3) is missing, the joint distribution for water level in gauges 1 and 2 (z_1 and z_2, respectively) is given by:

$$\begin{bmatrix} z_1 \\ z_2 \end{bmatrix} \sim N\left(\begin{bmatrix} \mu_1 \\ \mu_2 \end{bmatrix}, \begin{bmatrix} a & b \\ b & e \end{bmatrix}\right)$$

Importantly, water level in gauge 1 (z_1) can be predicted based on water level in gauge 2 (z_2) alone (i.e., ignoring the missing rainfall variable [z_3]) using the following expression:

$$p(z_1|z_2) = N(\beta_0^*+\beta_2^* z_2,\sigma^{2*})$$

where $\beta_0^*=\mu_1-\frac{b}{e}\mu_2, \beta_2^*=\frac{b}{e}$ and $\sigma^{2*}=a-\frac{b^2}{e}$. This expression demonstrates that, even if data from one or more on predictor variables are missing (e.g., z_3), the multivariate normal distribution assumption enables the prediction of z_1 based on the subset of variables that are not missing (e.g., z_2). Importantly, the regression coefficient for z_2 need not be the same when z_3 is observed versus when z_3 is missing (i.e., β_0, β_2 might be different from β_0^*, β_2^*). This feature of the multivariate normal distribution allows for straight-forward predictions based on "gappy data" without the need to first eliminate observations with missing data or develop gap-filled datasets.

2.4. Gaussian Copula (GC) models

The Gaussian Copula is a joint model for all observed variables (e.g., water level at different gauges and rainfall and other climate variables in different weather stations). Let the observed variable i at time t be denoted by $y_i^{(t)}$. Following Genest et al. (1995), we ensure that all the variables have a normal marginal distribution by using the following semiparametric transformation on the original variable $y_i^{(t)}$:

$$z_i^{(t)} = \Phi^{-1}\left(\hat{F}_i\left(y_i^{(t)}\right)\right)$$

where $\Phi(x)$ is the standard normal cumulative distribution function (CDF) and $\hat{F}_i(q)$ is the empirical CDF, given by:

$$\hat{F}_i(q) = \frac{1}{n_i+1}\sum_{t=1}^{n_i} I\left(y_i^{(t)}<q\right)$$

where n_i is the number of observations for variable i. We further assume a multivariate normal distribution for the vector of transformed

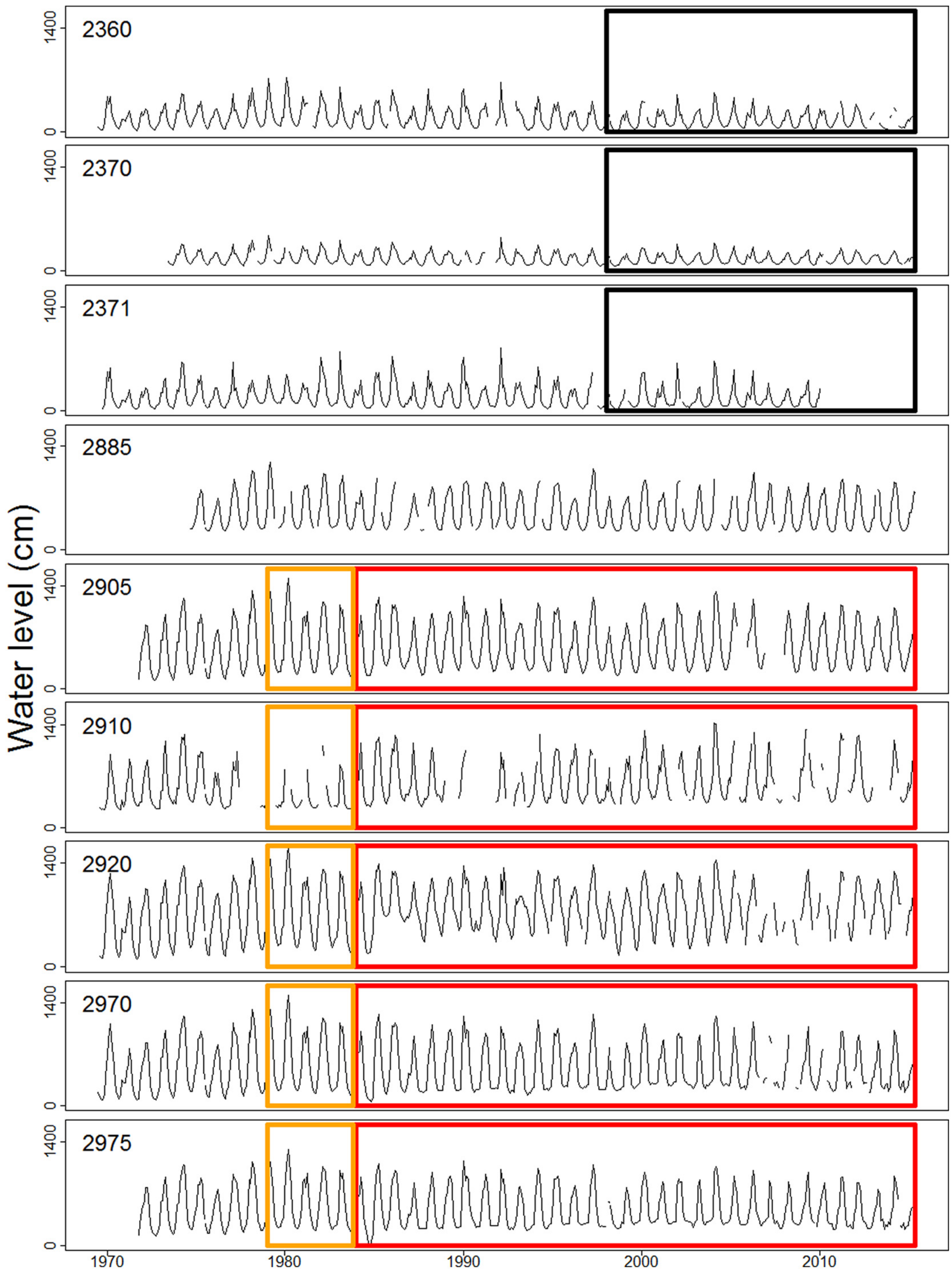

Fig. 3. Time series of water level measured at nine gauges on the Tocantins River and its tributaries. Numbers in the top left of each panel refer to river gauge identifiers (see Fig. 1). Colored boxes depict periods when data were excluded for model fitting. Orange boxes represent the model validation period (1979–1984) for sites likely impacted by the Tucuruí Dam. Red boxes represent the counterfactual period (1984–2015) for sites likely impacted by Tucuruí. Black boxes represent data that were potentially influenced by the Serra da Mesa dam and other newer dams upstream from Tucuruí. All data outside of these boxes were used for model calibration. (For interpretation of the references to color in this figure legend, the reader is referred to the web version of this article.)

variables at time t $\boldsymbol{z}^{(\boldsymbol{t})}_{p\times 1}$:

$$\boldsymbol{z}^{(\boldsymbol{t})}_{p\times 1} \sim N\left(\boldsymbol{\mu}_{\mathrm{p}\times 1}, \boldsymbol{\Sigma}_{\mathrm{p}\times \mathrm{p}}\right)$$

where $\boldsymbol{\mu}$ is a vector with the mean of each variable, $\boldsymbol{\Sigma}$ is the covariance matrix, and p is the overall number of variables. To capture potential delayed effects of climate variables and water level in control gauges (Villar et al., 2009), we used all of these variables with and without a one-month time lag (Costa et al., 2003). As a result, the overall number of variables was equal to $p = 53$. Finally, we adopted the following priors:

$$\boldsymbol{\mu}_{\mathrm{p}\times 1} \sim \mathrm{N}\left(\boldsymbol{0}_{p\times 1}, \mathbf{I}_{p\times p}\right)$$

$$\boldsymbol{\Sigma}^{-1}_{p\times p} \sim \text{Wishart}(v_0, \boldsymbol{M}_{p\times p})$$

where v_0 was set to the total number of variables plus two (i.e, $v_0 = p + 2$) and $\boldsymbol{M}$ was set to the identity matrix. The Wishart distribution is a commonly used prior for the precision matrix $\boldsymbol{\Sigma}^{-1}$ because of its conjugacy with the multivariate normal distribution and these choices for the prior parameters v_0 and $\boldsymbol{M}$ correspond to a relatively uninformative prior for $\boldsymbol{\Sigma}$ (Hoff, 2009).

To fit the model, we created a customized Gibbs sampler in R (R Core Team, 2013). A total of 10,000 iterations were run and the first half was discarded as burn-in. Convergence was visually assessed through trace plots of the log-likelihood and individual elements in $\boldsymbol{\mu}_{p\times 1}$. We make our code publicly available as Supporting Information, together with a short-tutorial on how to use it.

2.5. Benchmark models

We compared the performance of the GC model to that of two benchmark methods. The first benchmark model (hereafter referred to as the "monthly average" model) used the monthly average of the observed water level prior to dam construction to predict the counterfactual (Hui et al., 2004). For the second benchmark model, we relied on a multiple linear regression approach. Because this model requires complete observations, only water-level at control gauges and regional precipitation data were used as predictor variables. We created the regional precipitation predictor by averaging precipitation data across all 10 stations for each month and year combination, ignoring missing observations. We did not include other climate variables (i.e., temperature, humidity, and evaporation) due to the amount of missing data in these observations (i.e., these variables had >13% of missing data even after combining data from both long-term weather stations to create regional level variables). This benchmark model is hereafter referred to as complete data multiple regression model (CDMR).

2.6. Performance metrics for model comparison

For all models, we summarized the out-of-sample predictive performance for the validation period using the empirical coverage of the 95% predictive interval and the Nash-Sutcliffe (NS) coefficient. The empirical coverage quantifies the proportion of times that the 95% predictive interval encompassed observed water levels. A model that adequately represents predictive uncertainty should have an empirical coverage that roughly matches the nominal coverage of 95%. The Nash-Sutcliffe model efficiency coefficient is calculated as $NSE = 1 - \frac{\sum_{t=1}^{T}(y_t^o - y_t^p)^2}{\sum_{t=1}^{T}(y_t^o - \overline{y}^o)^2}$, where y_t^o and y_t^p are the observed and predicted water-levels at time t, respectively, and $\overline{y}^o = \frac{\sum_{t=1}^{T} y_t^o}{T}$ is the mean observed water-level. The NSE coefficient is a commonly used metric to assess predictive skill of hydrologic models, with a result of 1 corresponding to a perfect match between modeled and observed river water level.

3. Results

3.1. Model validation

The Nash-Sutcliffe coefficients for the GC model in the validation period were substantially higher those for the monthly average benchmark model, indicating that the GC model predicted more than just the highly seasonal pattern of water level variation (Table 1). The GC model had a similar predictive performance when compared to the CDMR model, except for gauge 2910, for which it had substantially improved performance than both the CDMR and monthly average benchmark models. In addition to improved performance for gauge 2910, the GC model was also able to make predictions for all 59 months of the validation period whereas the CDMR model, despite relying on a much smaller subset of predictors, was only able to make predictions for 49 months (83%) due to missing data on one or more predictor variables. Importantly, the GC model also more faithfully represented predictive uncertainty, with empirical coverage very close to the nominal coverage of 95% (Table 1) during the validation period. This is a critical model performance metric if the identification of impacts is predicated on the detection of statistically significant departures from the counterfactual. On the other hand, the CDMR approach yielded 95% predictive intervals that were too narrow (i.e., empirical coverage much lower than the nominal value of 95%) or too wide (i.e., empirical coverage equal to 100%). This reduced ability to adequately represent uncertainty is likely due to the lower number of complete data observations available to calibrate the CDMR model (38 observations for gauge 2910 and 50 for the remaining gauges). The GC model, on the other hand, yielded much better uncertainty characterization because it estimated its covariance matrix using (a) climate data from all 551 months (i.e., data depicted in Fig. 2), (b) pre-dam water-level data from impacted gauges, and (c) water-level data from control gauges for the entire period (i.e., the water-level data outside the boxes in Fig. 3).

Table 1
The GC model had substantially higher out-of-sample predictive skill for gauge 2910 and consistently outperformed the complete data multiple regression (CDMR) model in representing predictive uncertainty, based on the pre-dam validation data. Model performance metrics are shown for the Gaussian Copula (GC), complete data multiple regression (CDMR), and monthly average models. The best model for each gauge and criterion is highlighted in bold. Higher values for the Nash-Sutcliffe coefficients indicate greater predictive skill while empirical coverage values closer to 0.95 indicate better uncertainty characterization. Data during the validation period that were outside the range of the data used to calibrate the models were excluded when computing these performance metrics.

Gauge	Nash-Sutcliffe coefficient			Empirical coverage		
	GC	CDMR	Monthly average	GC	CDMR	Monthly average
2905	0.98	**0.99**	0.83	**0.95**	0.88	–
2910	**0.83**	0.60	0.68	**0.93**	0.92	–
2920	**0.98**	0.97	0.84	**0.95**	1.00	–
2970	**0.98**	**0.98**	0.80	**0.96**	0.83	–
2975	0.97	**0.98**	0.84	**0.96**	0.85	–

We determined the relative importance of each group of predictor variables (e.g., water-level from control gauges, rainfall from multiple stations, humidity from both weather stations, etc.) for the GC model by making predictions based solely on each group of variables and calculating the corresponding NS coefficient for the validation period. Models with only water-level data from control gauges yielded the highest NS coefficients for the validation period while models with only humidity covariates had the worst performance (Fig. 4). On the other hand, models with only temperature (including minimum, average, and maximum temperatures), rainfall, or evaporation variables generally resulted in similar NS coefficients. Interestingly, except for gauge 2910, there was almost no performance difference between models with only water-level data from control gauges and models containing both water-level and climate variables. While this might be interpreted as suggesting that climate variables have little predictive skill once data from control gauges are taken into account, these climate variables were actually critical for improving model performance when only data from gauge 2885 were available (results not shown). This situation corresponds to the time period after the upstream Serra da Mesa dam started to operate and water-level data from gauges 2360, 2370, and 2371 could no longer be used for prediction of the counterfactual (black rectangles in Fig. 3). These results highlight the ability and flexibility of the GC model in predicting water-level at impacted gauges by augmenting limited data from control gauges with climate data.

3.2. Dam operation period

After the pre-dam validation period and the initiation of operations at Tucuruí (i.e., from 1984 onwards), there were substantial

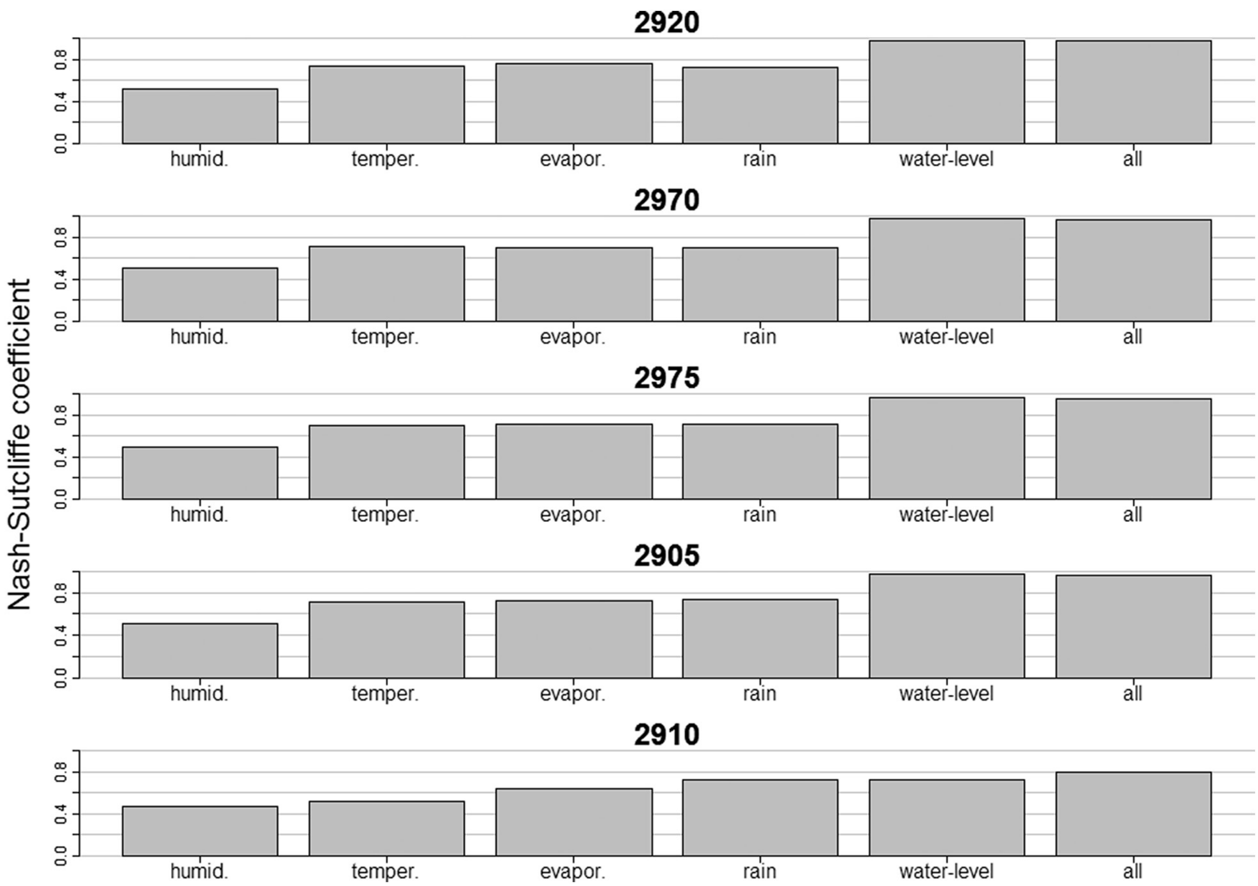

Fig. 4. Nash-Sutcliffe coefficients of models containing different subsets of predictor variables for the validation period. Humidity (humid.), evaporation (evapor.), and temperature (temper.) consist of data from two weather stations. Temperature data include minimum, average, and maximum temperatures. Rainfall data (rain) include information from ten stations and water-level data (water-level) contain pre-dam information from four gauges (gauges 2885, 2360, 2370, 2371; Fig. 1). Results for the model with all predictor variables are denoted by "all".

discrepancies between GC model predictions and observations, which can be attributed to the impact of dam operation on the hydrologic regime (Fig. 5). Specifically, results for the most downstream gauge (gauge 2975; Fig. 5a) revealed that water levels were significantly lower than predicted in the dry season immediately after the Tucuruí dam started to operate. In contrast, the primary impact of the dam in all subsequent years has been higher-than-expected water levels during the entire dry season, with only sporadic observations outside of the 95% credible interval during other periods. A very similar pattern can also be observed for the other downstream gauge located closest to Tucuruí (gauge 2970; Fig. 5b).

Dam impacts for the closest upstream gauge (gauge 2920; Fig. 5c) were of a somewhat different nature. After the first year of dam operation, dry-season water levels remained extremely high relative to the pre-dam expectation, with a particularly strong effect in the initial years of dam operation. This is likely a consequence of the proximity of this gauge to the dam reservoir, which precluded dry-season drawdown once the reservoir was full. We also found a subtler effect on the timing of water level decrease after wet season peaks. In general, water level declines were delayed and took longer than would be expected under the pre-dam condition. This phenomenon was consistent across multiple years, as indicated by the red dots on the falling limb of the hydrograph in most years (Fig. 5c). These higher-than-expected water levels during the low-water season and changes in the seasonality of drawdown were also evident in gauge 2905 (Fig. 5d), despite being >176 km away from the Tucuruí dam. Finally, there were also substantial discrepancies between observed and predicted water levels for gauge 2910 (Fig. 5e), located at an upstream tributary (Fig. 1). While these results should be viewed with caution given the lower predictive ability of the model for this gauge (NS = 0.83; Table 1) and relative sparseness of post-dam data, they mirror the response of all other upstream stations and are concordant with changes induced by backwater effects from increased water levels at the tributary's confluence with the Tocantins River.

While the significant deviations between observed and predicted river water level (red circles in Fig. 5) might be attributed to declining model performance as predictions are made further into the future (e.g., due to changes in other factors not included in our model), this is unlikely for two reasons. First, when we re-ran our algorithm with predictions starting in 1984 (instead of 1979), discrepancies were still evident immediately after 1984 and their temporal pattern at each site did not change substantially (data not shown). Second, if predictive model performance were declining with time one would expect the number of significant departures to increase over time. However, significant differences arise immediately after Tucuruí started to operate and the detected patterns do not vary substantially from year to year for impacted gauges throughout the first decade of dam operation.

Fig. 6 illustrates the magnitude of hydrological alteration attributable to Tucuruí for two specific metrics: dry season water level and timing of drawdown. Specifically, the left panels in Fig. 6 illustrate that observed dry-season water-levels in the post-dam period were 86 cm to 203 cm higher than those predicted by the GC model, while this difference ranged from −1 to 32 cm prior to dam operation. The right panels in Fig. 6 show that, after the dam started to operate, observed water-levels generally declined to pre-dam annual mean levels one month later than predicted for all gauges except for 2970 and 2920; for the gauge immediately downstream of Tucuruí (2970) there was little difference in the timing of water-level decline, but for the gauge

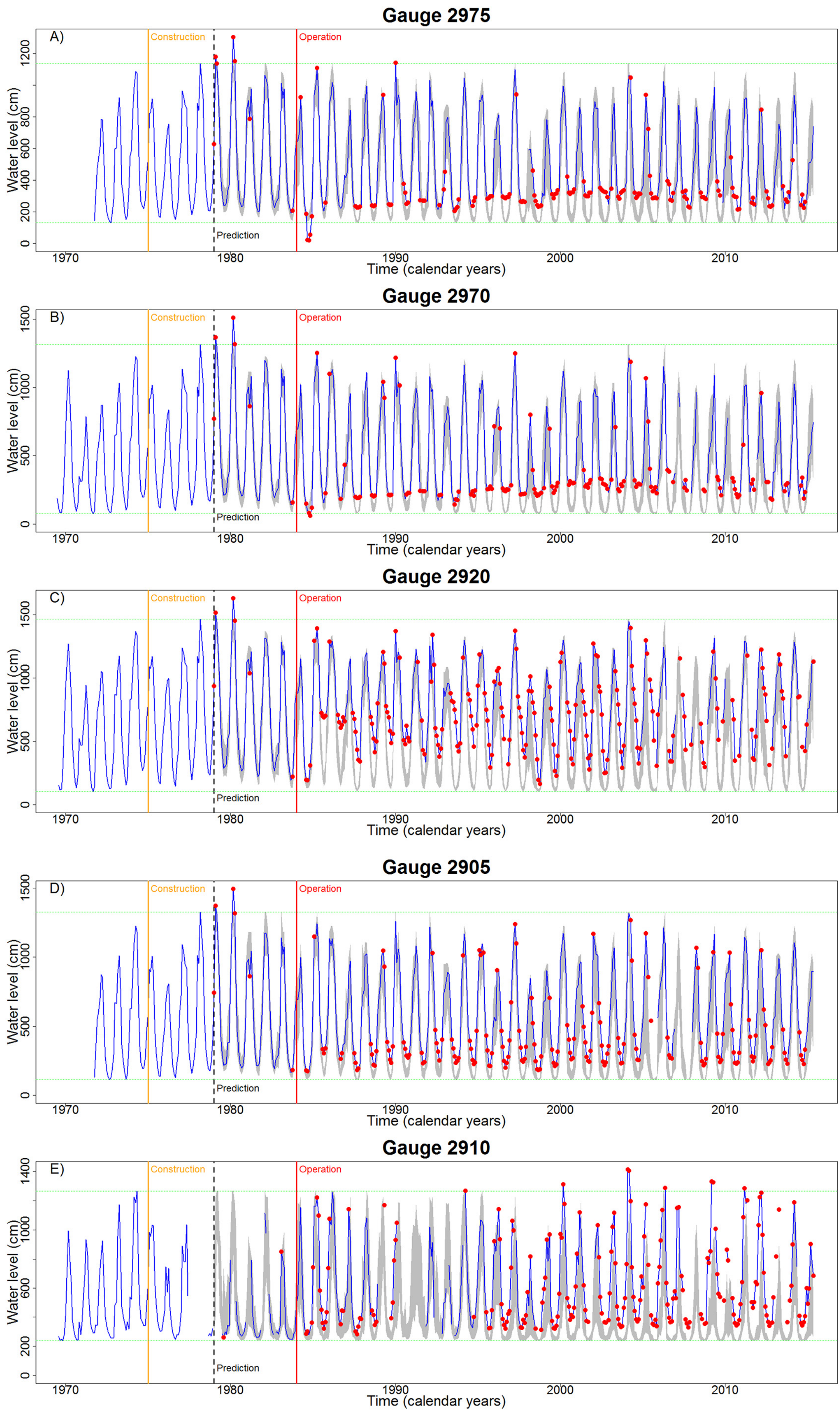
Gauge 2975
A)
Construction
Operation
Prediction
Water level (cm)
0
200
400
600
800
1200
1970
1980
1990
2000
2010
Time (calendar years)
Gauge 2970
B)
Construction
Operation
Prediction
Water level (cm)
0
500
1000
1500
1970
1980
1990
2000
2010
Time (calendar years)
Gauge 2920
C)
Construction
Operation
Prediction
Water level (cm)
0
500
1000
1500
1970
1980
1990
2000
2010
Time (calendar years)
Gauge 2905
D)
Construction
Operation
Prediction
Water level (cm)
0
500
1000
1500
1970
1980
1990
2000
2010
Time (calendar years)
Gauge 2910
E)
Construction
Operation
Prediction
Water level (cm)
0
200
600
1000
1400
1970
1980
1990
2000
2010
Time (calendar years)

immediately upstream of Tucuruí (2920), water-level declines were typically delayed by three months.

4. Discussion

In this paper, we present a Gaussian Copula (GC) approach to determine the impacts of dams on riverine hydrology. This approach avoids the stationarity assumption inherent to before and after comparisons and circumvents issues associated with incomplete and sparse time-series data, a ubiquitous challenge when integrating multiple time-series datasets, particularly in developing countries. While numerous physical and statistical methods are available for hydrological prediction, the GC method is a relatively straight-forward and flexible approach that captures uncertainty associated with data gaps and predictions within a single modeling step, which is critical for identifying impacts based on statistically significant differences between observations and predictions. In this work, we demonstrate how GC models can be used to yield insights into the impacts of dams on riverine hydrology and propose that the method is particularly valuable for locations with substantial data gaps.

4.1. Implications of inferred hydrologic alternation

We illustrate the utility of the GC approach by evaluating the impact of the Tucuruí dam on the hydrology of the Tocantins River in the Brazilian Amazon. Unsurprisingly, model results revealed clear and pervasive up- and downstream dam impacts on riverine hydrology. Similar to findings from the Mekong (Cochrane et al., 2014), we found consistently higher dry-season water levels for both upstream and downstream gauges after dam construction. These results suggest that low-lying areas that were seasonally dry before dam construction are likely to be flooded for longer periods of time or even permanently, a commonly observed phenomenon on dammed rivers (e.g., Forsberg et al., 2017; Poff and Olden, 2017). Beyond increased flooding, these hydrological changes represent a major disturbance of the flood pulse (Junk et al., 1989), with consequences for nutrient and sediment transport (Schindler and Smits, 2017), aquatic habitat availability and distribution (Richter et al., 1997), and river/floodplain biogeochemistry (Campo and Sancholuz, 1998) and geomorphology (Park and Latrubesse, 2017). In particular, the loss of dry season water level minima restricts floodplain colonization by taxa that require seasonal drawdown for successful reproduction (Kaplan et al., 2010), while longer and deeper flooding alters river and floodplain biogeochemical cycling by promoting the production and efflux of methane (dos Santos et al., 2017; Kemenes et al., 2007; Sawakuchi et al., 2014).

In additional to substantially higher water-levels during the dry season, upstream gauges also showed a substantial shift in the timing and rate of drawdown after the annual pulse, as well as a longer duration of high-water conditions. Changes in the magnitude, timing, and duration of annual extrema have been shown to disrupt fish spawning cues (Næsje et al., 1995) and negatively impact fish recruitment and production in the Amazon and other tropical rivers (Sabo et al., 2017; Suzuki et al., 2009). Beyond affecting habitat, seasonal water level changes also alter fish catchability and effort (Isaac et al., 2016; Lima et al., 2017), suggesting that the observed dam impacts on water level and seasonality likely impact local livelihoods and economies connected to ecosystem function. The hydrologic impact of the dam was evident as far as 176 km away from the dam (gauge 2905), highlighting the widespread impacts of dams even far from the directly impacted reservoir area. There were also signs of potential impact in a tributary of the Tocantins (gauge 2910). While data sparsity and model limitations do not support unequivocal attribution of these discrepancies to the Tucuruí dam, these tributary impacts are most likely due to backwater effects from increased dry-season water-levels in the Tocantins River.

These results are concordant with the analysis by Timpe and Kaplan (2017), who used the Indicators of Hydrologic Alteration (IHA) method (Richter et al., 1996) to quantify dam-induced hydrologic change in the Brazilian Amazon and analyzed many of the gauges used in this study (from downstream to upstream: 2970, 2920, 2905, 2885, 2370, and 2360; Fig. 1). As in our study, Timpe and Kaplan (2017) found large and significant impacts to the hydrologic regime from the Tucururí dam for gauges 2970 and 2920 (i.e., the closest downstream and upstream gauges), with overall hydrologic alteration (HA) of 39 and 25%, respectively. Downstream of the dam (gauge 2970), Timpe and Kaplan (2017) found the largest flow regime changes for IHA groups 2, 4 and 5, which describe the magnitude and duration of annual low- and high-water conditions, the frequency and duration of high and low pulses, and the rate and frequency of water condition changes, respectively. Specifically, within IHA group 2, they saw the largest downstream changes in flow minima (increases of 71, 72, 69, and 60% for the 1-, 3-, 7-, 30-, and 90-day minima) and only small changes (<20%) for all measures of flow maxima (Timpe, 2016). Other large and significant changes detailed in Timpe (2016) include increases in low pulse count and duration (group 4) of 200 and 93%, respectively, and an increase in the number of reversals (group 5) by 160%. While these results are not directly comparable to our study due to differences in temporal resolution (i.e., daily data for IHA and monthly data here which preclude, for example, estimating reversals), they mirror our findings of important downstream changes to flow metrics dominated by increased dry-season water level and flow (Figs. 5a–b and 6).

Upstream of the dam (gauge 2920), Timpe and Kaplan (2017) reported the greatest changes in IHA groups 1, 2, and 4, where group 1 describes the magnitude of monthly flows, and the other two groups are noted above. For group 1, Timpe (2016) lists the largest changes for median monthly flows in June through October (increases of 29, 81, 119, 74, and 33%), which correspond to the higher-than-expected water levels we identified during falling limbs and dry seasons (Figs. 5c and 6). As with downstream gauge 2970 and concordant with our results, Timpe (2016) also notes substantial increases in flow minima (31 to 42%) and smaller changes (<20%) in maxima, all of which are consistent with increased water levels caused by backwater from the maintenance of surface water elevation in the reservoir. Finally, Timpe and Kaplan (2017) found hydrologic alteration at gauge 2905 to be relatively low (overall HA of 10%), whereas our results indicate significant increases in water levels during the low-water season and altered flow seasonality (Figs. 5d and 6). This difference suggests that, in addition to circumventing stationarity issues inherent in IHA, the GC approach may also be able to identify important hydrological changes that indicator methods like IHA may not identify.

Defining what represents an "acceptable" level of hydrological alteration across river systems and for a range of ecosystem services and impacted species remains an overarching challenge in ecohydrology (Poff and Zimmerman, 2010; Williams, 2018). While comprehensive flow-ecology frameworks like the Ecological Limits of Hydrological Alteration (ELOHA) method (Poff et al., 2010) provide a robust framework to organize hydrologic information, their ability to empirically connect flow regime and ecosystem response has been mixed (McManamay et al., 2013), and they have been most successful for connecting flow alteration and aquatic invertebrate communities (e.g., Solans and Garcia de Jalon, 2016). Moreover, in regions where biological data are scarce,

Fig. 5. Comparison of counterfactual predictions (grey shaded regions) and observed water level (blue line) for five gauges (ordered top to bottom from downstream to upstream of the Tucuruí dam). The yellow and red vertical lines depict the initiation and completion of the Tucuruí dam construction, respectively. The dashed black vertical line depicts the end of the data used to train the model and the beginning of the prediction period. The period between the black and red lines corresponds to the validation period. Observations that do not fall between the 95% counterfactual credible intervals are highlighted with red circles. Green horizontal lines show the range of the data used to train the model. (For interpretation of the references to color in this figure legend, the reader is referred to the web version of this article.)

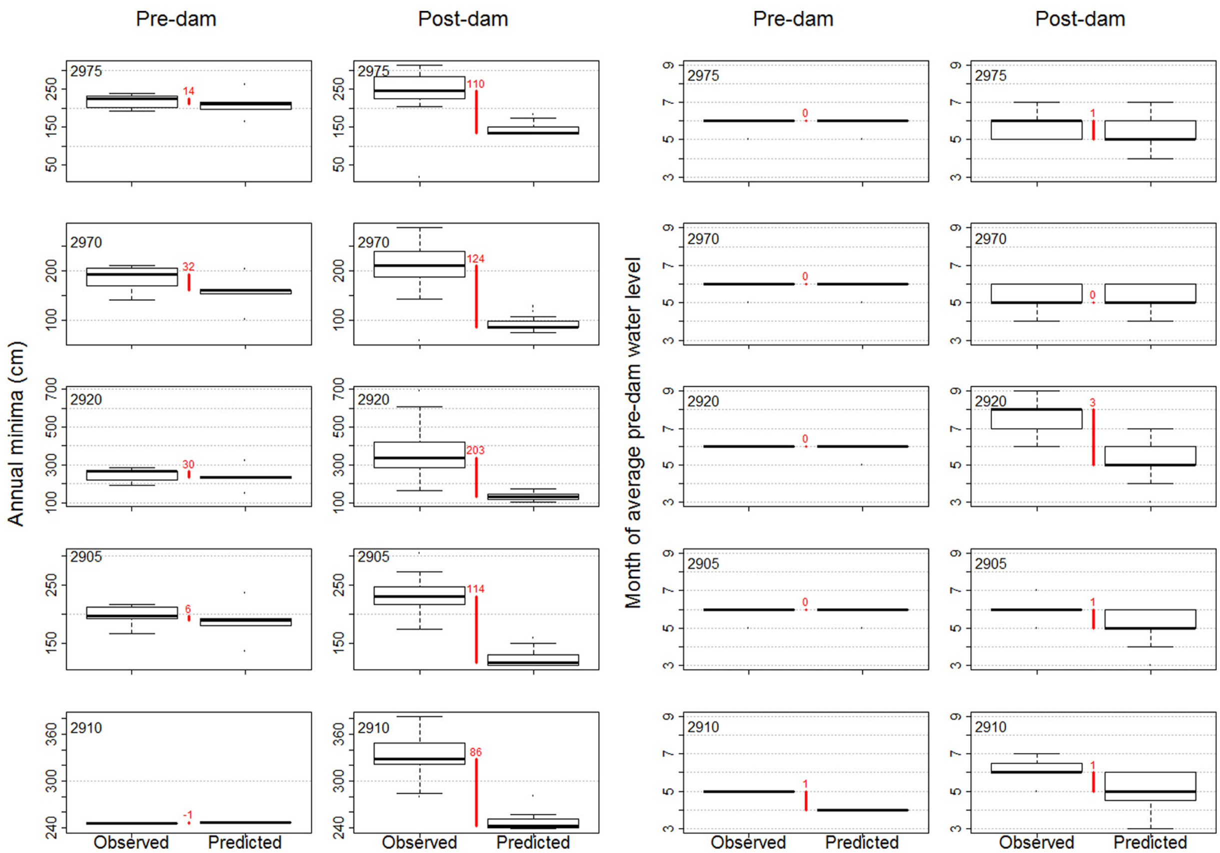

Fig. 6. Comparison of counterfactual predictions and observations for water level during the dry season (left panels) and timing of water-level decline (right panels) for five gauges (ordered top to bottom from downstream to upstream of the Tucuruí dam). Red lines and numbers depict the difference in median observed and predicted values. Results are shown separately for the pre-dam and post-dam operation periods and are based only on years with water-level data for all 12 months. (For interpretation of the references to color in this figure legend, the reader is referred to the web version of this article.)

hydrologic alteration methods may be the only tool available (Timpe, 2016). In this context, the question of how much dry season water levels can increase and drawdown timing be altered in the Tocantins without negatively affecting the ecosystem depends largely on what ecosystem element is considered and remains an open question. Some of the most pervasive and detrimental changes to riverine ecology on the Tocantins have been from losses to fish diversity and fisheries production (Akama, 2017; de Mérona et al., 2001; Ribeiro et al., 1995), which are likely driven by both flow alteration and disruption of medium- and long-distance fish migration (e.g., Winemiller et al., 2016). Additional research is required to better understand the combined effects of flow alteration and riverine fragmentation on riverine ecology (Anderson et al., 2018).

4.2. Comparison to standard impact assessment methods

The main advantage of before and after comparisons is their simplicity and ease of interpretation. Applications of this approach have provided considerable insights regarding hydrologic alterations induced by dams across the Brazilian Amazon (e.g., Timpe and Kaplan, 2017) the United States (Magilligan and Nislow, 2005; Pyron and Neumann, 2008; Richter et al., 1998), and around the globe (Maingi and Marsh, 2002; Schneider et al., 2013; Yang et al., 2012). However, besides the questionable validity of the stationarity assumption (as evidenced by the long-term trends in precipitation, land use/land cover, and river discharge in the region, reported elsewhere; Coe et al., 2011; Nobre et al., 2016; Silverio et al., 2015), these comparisons also often require relatively long-term and complete datasets. For example, studies from arid and temperate climates suggest using at least 20 years of pre- and post-dam data (Richter et al., 1997). Timpe and Kaplan (2017) showed that the record length required for before and after comparisons in the Amazon can be as long as 37 years, with longer records required for lower-flow and higher-elevation rivers. Critically, the approach we propose here can be used to identify statistically significant alteration immediately following an impact, without requiring any prescribed length of post-impact data.

To avoid the stationarity assumption inherent to IHA and other indicator-based methods, regression models have been extensively used to predict river water-level based on climate and water-level variables (Brown et al., 2005; Scott and Lesch, 1997). However, these regression models can have limited utility in situations with substantial missing data on predictor variables. For example, while the complete data multiple regression (CDMR) approach performed relatively well for all but one station based on the Nash-Sutcliffe coefficient, this model was only able to make 83% of the required predictions during the validation period and resulted in 95% predictive intervals with poor coverage compared to the GC model (Table 1). One potential alternative approach to the missing-data problem is to rely on a two-stage procedure, in which data gaps in covariates are first filled and then a multiple regression approach with the filled covariates is used to make predictions of the counterfactual. However, coherently propagating the uncertainty associated with these imputed values to the final predictions of water-level is not straightforward in this two-stage procedure. In contrast to these two-stage methods, the GC approach coherently captures the uncertainty associated with data gaps and predictions within a single modeling step, which is critical if the goal is to identify dam impact based on statistically significant differences between observations and predictions.

An alternative way to assess impact on riverine hydrology is to use physically-based rainfall-runoff models (Devi et al., 2015). While there are well-acknowledged issues with the application of physical models for hydrologic prediction (e.g., Beven, 1989; Beven, 1993), spatially distributed, numerical watershed models have been widely applied to simulate spatiotemporal streamflow dynamics for decades, including in the Amazon (Coe, 2000; Coe et al., 2008; Lima et al., 2014; Pontes et al., 2017; Sorribas et al., 2016). Properly calibrated and validated physically based watershed models (Calver, 1988) inherently avoid the stationarity assumption and could be used to predict counterfactual river flows and levels in dammed systems. However, watershed models require substantial effort, data, and specialized expertise to build, verify, and run (Korfmacher, 2001). The investment in time, personnel, and data required to develop and apply these models often exceeds available resources in regions where EIAs are being carried out, and in some cases, the required data are simply not available. For example, most standardized land use/land cover remote sensing products for the Amazon region only cover from 2000 onwards (e.g., Hansen et al., 2013; INPE, 2018; MAPBIOMAS, 2018), precluding their use for the Tucuruí dam. Importantly, existing physical models developed for the Amazon have not taken dam operation into consideration. In this context, a statistical method like the proposed GC model might be an attractive option, given that it is more straight-forward to implement (when compared to a physically-based rainfall-runoff models), while also requiring less data. While the GC model has been applied here to a single case of altered hydrology, this approach is potentially useful for determining the counterfactual in impact assessments of any time structured variable.

4.3. Model limitations

There are several potential limitations of our method for assessing dam impacts. First, the semi-parametric approach that we adopt to ensure that each variable is marginally normally distributed restricts predictions to be within the range of the data used to train the model. We do not view this as a critical limitation because, in our case study, most of the discrepancies between the observed and predicted water levels detected were well within the range of the training data. Second, high collinearity between predictor variables is often an important concern when applying regression models. However, we note that high collinearity is problematic when the research goal is attribution (i.e., determining how each predictor variable influences the response variable). Given our focus on assessing impacts, our primary interest is in model prediction rather than attribution, limiting this issue in our context. Moreover, collinearity does not necessarily decrease predictive skill (Morrissey and Ruxton, 2018), as evidenced by the high out-of-sample predictive ability of the GC model for the validation period (Table 1).

Third, we assume that climate variables (temperature, humidity, and rainfall) are not impacted by dams or their reservoirs, however it has been suggested that the construction of dams can increase deforestation rates, which in turn may potentially reduce regional rainfall (Stickler et al., 2013). We believe that accounting for this indirect dam impact on river hydrology and ecology is an important area for future research but is beyond the scope of this work. Fourth, similar to BACI designs, our method relies on the identification of appropriate control gauges. This is not a simple task, given that dam-induced changes in the hydrologic regime may occur even at long distances from the dam (e.g., gauge 2905, which is 176 km away from Tucuruí). During preliminary analysis, we experimented with different sets of potentially impacted gauges and examined the corresponding model results to see if there were clear signs of dam impact. In general, we took a conservative approach, preferring to err on the side of assuming more gauges were potentially impacted, because this is less likely to bias the impact evaluation than incorrectly assigning a truly impacted gauge as a control gauge. Nevertheless, additional research is needed to develop methods to robustly identify suitable control gauges.

The fifth limitation of our study is a lack of consideration for land-use land-cover (LULC) change in the region, given that LULC is a primary mediator of the relationship between rainfall and river flow (Costa et al., 2003). Indeed, there has been widespread clearing of native vegetation in this watershed and both empirical observations and numerical modeling throughout the region suggest that these LULC changes reduce evapotranspiration, increase river discharge, and changed flow seasonality (Coe et al., 2011; Silverio et al., 2015). Unfortunately, most standardized LULC remote sensing products for the region only cover from 2000 onwards (e.g., Hansen et al., 2013; INPE, 2018; MAPBIOMAS, 2018), precluding their use in our models. Nevertheless, we believe that some LULC effects are probably captured indirectly in the water level data from control gauges. Furthermore, we also note that large-scale LULC changes likely to impact river water level are slow when compared to the abrupt changes immediately upon dam operation depicted in Fig. 5, suggesting that the discrepancies between predicted and observed water levels in the years immediately following dam operation are unlikely to be attributable to LULC changes.

5. Conclusions

Giving the global boom in hydropower dam construction (Anderson et al., 2018; Finer and Jenkins, 2012; Winemiller et al., 2016; Zarfl et al., 2015), improving our understanding of how dams influence river hydrology, and consequently impact riverine ecohydrology and ecosystem services, will be increasingly important for preventing and mitigating these impacts. We propose and apply a Gaussian Copula (GC) model to quantify the environmental impact associated with the Tucuruí dam, a method that successfully circumvents substantial data gaps and the stationary assumption inherent to many environmental impact assessment methods. The comparison of the predicted to the observed water-level for the post-dam period reveals that the Tucuruí dam resulted in substantial alteration of the flood pulse, with much higher dry-season water levels both upstream and downstream of the dam and delayed and extended duration of wet-season drawdown. Future research could focus on determining the generalizability of these findings for other large dams in the region, while accounting for land-use/land-cover change, and developing methods to more objectively determine control gauges. Flexible statistical models like GC models provide the ability to combine disparate time-series data to rapidly assess and attribute hydrologic changes to infrastructure and other anthropogenic phenomena in regions where data and/or physical modeling expertise are scarce and thus have wide utility for quantifying these impacts on riverine hydrology worldwide.

Declarations of conflict of interest

None.

Acknowledgments

This work was partly supported by the Water Institute at the University of Florida. The funders had no role in study design, data collection and analysis, decision to publish, or preparation of the manuscript. We thank the numerous comments and suggestions made by Marcia Macedo, Michael Coe, and Elineide Marques. Water-level and precipitation data can be found in Tucker Lima et al. (2016) while the remaining meteorological data (relative humidity, evaporation, minimum, maximum, and mean temperatures) are available at http://www.inmet.gov.br/portal/. All the data are freely available. Code to fit the GC model is provided in the Supporting Information, together with a short-tutorial on how to use it.

Appendix A. Supplementary material

Supplementary data to this article can be found online at https://doi.org/10.1016/j.scitotenv.2019.04.377.

References

Abadie, A., Diamond, A., Hainmueller, J., 2010. Synthetic control methods for comparative case studies: estimating the effect of California's tobacco control program. J. Am. Stat. Assoc. 105 (490), 493–505.

Akama, A., 2017. Impacts of the hydroelectric power generation over the fish fauna of the Tocantins river, Brazil: Maraba dam, the final blow. Oecologia 21 (3), 222–231.

Anderson, E.P., et al., 2018. Fragmentation of Andes-to-Amazon connectivity by hydropower dams. Sci. Adv. 4 (1), eaao1642.

Andersson, J.C.M., Zehnder, A.J.B., Wehrli, B., Yang, H., 2012. Improved SWAT model performance with time-dynamic Voronoi tessellation of climatic input data in Southern Africa. J. Am. Water Resour. Assoc. 48 (3), 480–493.

Beighley, R.E., et al., 2009. Simulating hydrologic and hydraulic processes throughout the Amazon River Basin. Hydrol. Process. 23 (8), 1221–1235.

Beven, K., 1989. Changing ideas in hydrology - the case of physically-based models. J. Hydrol. 105, 157–172.

Beven, K., 1993. Prophecy, reality and uncertainty in distributed hydrological modelling. Adv. Water Resour. 16 (1), 41–51.

Brown, A.E., Zhang, L., McMahon, T.A., Western, A.W., Vertessy, R.A., 2005. A review of paired catchment studies for determining changes in water yield resulting from alterations in vegetation. J. Hydrol. 310 (1), 28–61.

Calver, A., 1988. Calibration, sensitivity and validation of a physically-based rainfall-runoff model. J. Hydrol. 103 (1–2), 103–115.

Campo, J., Sancholuz, L., 1998. Biogeochemical impacts of submerging forests through large dams in the Rio Negro, Uruguay. J. Environ. Manag. 54 (1), 59–66.

Castello, L., Macedo, M.N., 2016. Large-scale degradation of AMazonian freshwater ecosystems. Glob. Chang. Biol. 22, 990–1007.

Cetra, M., Petrere Jr, M., 2001. Small-scale fisheries in the middle River Tocantins, Imperatriz (MA), Brazil. Fish. Manag. Ecol. 8 (2), 153–162.

Clausen, J.C., Spooner, J., 1993. Paired Watershed Study Design. Environmental Protection Agency, Washington, DC (United States) (Office of Wetlands, Oceans and Watersheds).

Cochrane, T.A., Arias, M.E., Piman, T., 2014. Historical impact of water infrastructure on water levels of the Mekong River and the Tonle Sap system. Hydrol. Earth Syst. Sci. 18, 4529–4541.

Coe, M.T., 2000. Modeling terrestrial hydrological systems at the continental scale: testing the accuracy of an atmospheric GCM. J. Clim. 13 (4), 686–704.

Coe, M.T., Costa, M.H., Howard, E.A., 2008. Simulating the surface waters of the Amazon River basin: impacts of new river geomorphic and flow parameterizations. Hydrol. Process. 22 (14), 2542–2553.

Coe, M.T., Latrubesse, E.M., Ferreira, M.E., Amsler, M.L., 2011. The effects of deforestation and climate variability on the streamflow of the Araguaia River, Brazil. Biogeochemistry 105 (1–3), 119–131.

Costa, M.H., Foley, J.A., 1999. Trends in the hydrologic cycle of the Amazon basin. J. Geophys. Res.-Atmos. 104 (D12), 14189–14198.

Costa, M.H., Botta, A., Cardille, J.A., 2003. Effects of large-scale changes in land cover on the discharge of the Tocantins River, Southeastern Amazonia. J. Hydrol. 283 (1), 206–217.

de Mérona, B., Dos Santos, G.M., De Almeida, R.G., 2001. Short term effects of Tucuruí Dam (Amazonia, Brazil) on the trophic organization of fish communities. Environ. Biol. Fish 60 (4), 375–392.

Devi, G.K., Ganasri, B.P., Dwarakish, G.S., 2015. A review on hydrological models. Aquat. Proc. 4, 1001–1007.

dos Santos, M.A., et al., 2017. Estimates of GHG emissions by hydroelectric reservoirs: the Brazilian case. Energy 133, 99–107.

Favre, A.-C., Adlouni, S.E., Perreault, L., Thiemonge, N., Bobee, B., 2004. Multivariate hydrological frequency analysis using copulas. Water Resour. Res. 40, 1–12.

Finer, M., Jenkins, C.N., 2012. Proliferation of hydroelectric dams in the Andean Amazon and implications for Anders-Amazon connectivity. PLoS One 7 (4), e35126.

Forsberg, B.R., et al., 2017. The potential impact of new Andean dams on Amazon fluvial ecosystems. PLoS One 12 (8), e0182254.

Genest, C., Ghoudi, K., Rivest, L.-P., 1995. A semiparametric estimation procedure of dependence parameters in multivariate families of distributions. Biometrika 82 (3), 543–552.

Getirana, A.C.V., et al., 2009. Hydrological monitoring of poorly gauged basins based on rainfall–runoff modeling and spatial altimetry. J. Hydrol. 379 (3), 205–219.

Hansen, M.C., et al., 2013. High-resolution global maps of 21st-century forest cover change. Science 342 (6160), 850–853.

Hao, Z., Singh, V.P., 2016. Review of dependence modeling in hydrology and water resources. Prog. Phys. Geogr. 40 (4), 549–578.

Hoff, P.D., 2009. A First Course in Bayesian Statistical Methods. Springer Texts in StatisticsSpringer, New York.

Hui, D., et al., 2004. Gap-filling missing data in eddy covariance measurements using multiple imputation (MI) for annual estimations. Agric. For. Meteorol. 121, 93–111.

INPE, 2018. Projeto PRODES. Instituto Nacional de Pesquisas Espaciais.

International Rivers, 2016. Araguaia & Tocantins Rivers. International Rivers, Berkeley, CA.

Isaac, V.J., Castello, L., Santos, P.R.B., Ruffino, M.L., 2016. Seasonal and interannual dynamics of river-floodplain multispecies fisheries in relation to flood pulses in the lower Amazon. Fish. Res. 183, 352–359.

Junk, W.J., Bayley, P.B., Sparks, R.E., 1989. The flood pulse concept in river-floodplain systems. Can. Spec. Publ. Fish. Aquat. Sci. 106 (1), 110–127.

Kaplan, D., et al., 2010. Linking river, floodplain, and vadose zone hydrology to improve restoration of a coastal river affected by saltwater intrusion. J. Environ. Qual. 39 (5), 1570–1584. https://doi.org/10.2134/jeq2009.0375.

Kemenes, A., Forsberg, B.R., Melack, J.M., 2007. Methane release below a tropical hydroelectric dam. Geophys. Res. Lett. 34 (12).

Korfmacher, K.S., 2001. The politics of participation in watershed modeling. Environ. Manag. 27 (2), 161–176.

Lima, L.S., et al., 2014. Feedbacks between deforestation, climate, and hydrology in the Southwestern Amazon: implications for the provision of ecosystem services. Landsc. Ecol. 29 (2), 261–274.

Lima, M.A.L., Kaplan, D.A., Doria, C.R.C., 2017. Hydrological controls of fisheries production in a major Amazonian tributary. Ecohydrology 10, e1899.

Liu, Z., et al., 2018. A framework for exploring joint effects of conditional factors on compound floods. Water Resour. Res. 54 (4), 2681–2696.

Magilligan, F.J., Nislow, K.H., 2005. Changes in hydrologic regime by dams. Geomorphology 71 (1), 61–78.

Maingi, J.K., Marsh, S.E., 2002. Quantifying hydrologic impacts following dam construction along the Tana River, Kenya. J. Arid Environ. 50 (1), 53–79.

MAPBIOMAS, 2018. MAPBIOMAS.

McManamay, R.A., Orth, D.J., Dolloff, C.A., Mathews, D.C., 2013. Application of the ELOHA framework to regulated rivers in the Upper Tennessee River Basin: a case study. Environ. Manag. 51 (6), 1210–1235.

Milly, P.C.D., et al., 2007. Stationarity is dead. Ground Water News & Views 4 (1), 6–8.

Moran, E.F., Lopez, M.C., Moore, N., Muller, N., Hyndman, D.W., 2018. Sustainable hydropower in the 21st century. Proc. Natl. Acad. Sci. U. S. A. 115 (47), 11891–11898.

Morrissey, M.B., Ruxton, G.D., 2018. Multiple regression is not multiple regressions: the meaning of multiple regression and the non-problem of collinearity. Philos. Theory Pract. Biol. 10 (3).

Næsje, T., Jonssons, B., Skudarl, J., 1995. Spring flood: a primary cue for hatching of river spawning Coregoninae. Can. J. Fish. Aquat. Sci. 52 (10), 2190–2196.

Nobre, C.A., et al., 2016. Land-use and climate change risks in the Amazon and the need of a novel sustainable development paradigma. Proc. Natl. Acad. Sci. U. S. A. 113 (39), 10759–10768.

Park, E., Latrubesse, E.M., 2017. The hydro-geomorphologic complexity of the lower Amazon River floodplain and hydrological connectivity assessed by remote sensing and field control. Remote Sens. Environ. 198, 321–332.

Poff, N.L., Olden, J.D., 2017. Can dams be designed for sustainability? Science 358 (6368), 1252–1253.

Poff, N.L., Zimmerman, J.K., 2010. Ecological responses to altered flow regimes: a literature review to inform the science and management of environmental flows. Freshw. Biol. 55 (1), 194–205.

Poff, N.L., Olden, J.D., Merritt, D.M., Pepin, D.M., 2007. Homogenization of regional river dynamics by dams and global biodiversity implications. Proc. Natl. Acad. Sci. U. S. A. 104 (14), 5732–5737.

Poff, N.L., et al., 2010. The ecological limits of hydrologic alteration (ELOHA): a new framework for developing regional environmental flow standards. Freshw. Biol. 55 (1), 147–170.

Pontes, P.R.M., et al., 2017. MGB-IPH model for hydrological and hydraulic simulation of large floodplain river systems coupled with open source GIS. Environ. Model Softw. 94, 1–20.

Pyron, M., Neumann, K., 2008. Hydrologic alterations in the Wabash River watershed, USA. River Res. Appl. 24 (8), 1175–1184.

R Core Team, 2013. R: A Language and Environment for Statistical Computing. R Foundation for Statistical Computing, Vienna, Austria.

Renard, B., Lang, M., 2007. Use of a Gaussian copula for multivariate extreme value analysis: some case studies in hydrology. Adv. Water Resour. 30, 897–912.

Ribeiro, M.C.L.d.B., Petrere, M., Juras, A.A., 1995. Ecological integrity and fisheries ecology of the Araguaia—Tocantins River Basin, Brazil. Regul. Rivers: Res. Manage. 11 (3–4), 325–350.

Richter, B.D., Baumgartner, J.V., Powell, J., Braun, D.P., 1996. A method for assessing hydrologic alteration within ecosystems. Conserv. Biol. 10 (4), 1163–1174.

Richter, B., Baumgartner, J., Wigington, R., Braun, D., 1997. How much water does a river need? Freshw. Biol. 37 (1), 231–249.

Richter, B.D., Baumgartner, J.V., Braun, D.P., Powell, J., 1998. A spatial assessment of hydrologic alteration within a river network. Regul. Rivers: Res. Manage. 14 (4), 329–340.

Rubin, D.B., 1976. Inference and missing data. Biometrika 63 (3), 581–592.

Ruelland, D., Ardoin-Bardin, S., Billen, G., Servat, E., 2008. Sensitivity of a lumped and semi-distributed hydrological model to several methods of rainfall interpolation on a large basin in West Africa. J. Hydrol. 361, 96–117.

Sabo, J.L., et al., 2017. Designing river flows to improve food security futures in the Lower Mekong Basin. Science 358, eaao1053.

Sawakuchi, H.O., et al., 2014. Methane emissions from Amazonian Rivers and their contribution to the global methane budget. Glob. Chang. Biol. 20 (9), 2829–2840.

Schindler, D.E., Smits, A.P., 2017. Subsidies of aquatic resources in terrestrial ecosystems. Ecosystems 20 (1), 78–93.

Schneider, T., 2001. Analysis of incomplete climate data: estimation of mean values and covariance matrices and imputation of missing values. J. Clim. 14, 853–871.

Schneider, C., Laize, C.L.R., Acreman, M.C., Florke, M., 2013. How will climate change modify river flow regimes in Europe? Hydrol. Earth Syst. Sci. 17, 325–339.

Scott, D.F., Lesch, W., 1997. Streamflow responses to afforestation with Eucalyptus grandis and Pinus patula and to felling in the Mokobulaan experimental catchments, South Africa. J. Hydrol. 199, 360–377.

Silverio, D.V., et al., 2015. Agricultural expansion dominates climate changes in southeastern Amazonia: the overlooked non-GHG forcing. Environ. Res. Lett. 10.

Solans, M.A., Garcia de Jalon, D., 2016. Basic tools for setting environmental flows at the regional scale: application of the ELOHA framework in a Mediterranean river basin. Ecohydrology 9 (8), 1517–1538.

Sorribas, M.V., et al., 2016. Projections of climate change effects on discharge and inundation in the Amazon basin. Clim. Chang. 136 (3–4), 555–570.

Stickler, C.M., et al., 2013. Dependence of hydropower energy generation on forests in the Amazon Basin at local and regional scales. Proc. Natl. Acad. Sci. U. S. A. 110 (23), 9601–9606.

Suzuki, H.I., et al., 2009. Inter-annual variations in the abundance of young-of-the-year of migratory fishes in the Upper Paraná River floodplain: relations with hydrographic attributes. Braz. J. Biol. 69 (2), 649–660.

Timpe, K., 2016. Quantifying the Ecohydrological Impacts of Damming the Amazon. University of Florida, Gainesville, Florida.

Timpe, K., Kaplan, D., 2017. The changing hydrology of a dammed Amazon. Sci. Adv. 3, e1700611.

Tucker Lima, J.M., et al., 2016. A social-ecological database to advance research on infrastructure development impacts in the Brazilian Amazon. Sci. Data 3, 160071. https://doi.org/10.1038/sdata.2016.71.

Tundisi, J.G., 2008. Recursos hidricos no futuro: problemas e solucoes. Estudos Avancados 22, 7–16.

Tundisi, J.G., Santos, M.A., Menezes, C.F.S., 2005. Tucurui Reservoir: Experience and Lessons Learned Brief. International Waters Learning Exchange & Resource Network.

van Buuren, S., Boshuizen, H.C., Knook, D.L., 1999. Multiple imputation of missing blood pressure covariates in survival analysis. Stat. Med. 18, 681–694.

Villar, J.C.E., et al., 2009. Contrasting regional discharged evolutions in the Amazon basin (1974–2004). J. Hydrol. 375 (3–4), 297–311.

Weiss, D.J., et al., 2014. An effective approach for gap-filling continental scale remotely sensed time-series. ISPRS J. Photogramm. Remote Sens. 98, 106–118.

Williams, J.G., 2018. Building hydrologic foundations for applications of ELOHA: how long a record should you have? River Res. Appl. 34 (1), 93–98.

Winemiller, K.O., et al., 2016. Balancing hydropower and biodiversity in the Amazon, Congo, and Mekong. Science 2016 (6269), 128–129.

Xu, K., Yang, D., Xu, X., Lei, H., 2015. Copula based drought frequency analysis considering the spatio-temporal variability in Southwest China. J. Hydrol. 527, 630–640.

Yang, Z., Yan, Y., Liu, Q., 2012. Assessment of the flow regime alterations in the Lower Yellow River, China. Eco. Inform. 10, 56–64.

Yin, J., et al., 2018. A copula-based analysis of projected climate changes to bivariate flood quantiles. J. Hydrol. 566, 23–42.

Zarfl, C., Lumsdon, A., Berlekamp, J., Tydecks, L., Tockner, K., 2015. A global boom in hydropower dam construction. Aquat. Sci. 77, 161–170.